Journal of Agrometeorology

(A publication of Association of Agrometeorologists)

ISSN : 0972-1665 (print), 2583-2980 (online)
Vol. No. 28 (2) : 150-158 (June - 2026)
https://doi.org/10.54386/jam.v28i2.3349
https://journal.agrimetassociation.org/index.php/jam

Research paper

Assessment of Hydrological Drought and Vegetation Cover Trend in the Iraqi Marshlands Using Remote Sensing and GIS

FADHAA TURKI DAKHIL[1], NURIDAH BINTI SABTU[1*], and ALAA G. KHALAF[2]

[1]*School of Civil Engineering, Universiti Sains Malaysia, Engineering Campus, 14300, Nibong Tebal, Penang, Malaysia*
[2]*Scientific Research Commission, Baghdad, Iraq*
[*]*Corresponding author email:* nsabtu@usm.my

ABSTRACT

The Iraqi marshlands are among the most important wetland ecosystems in the country because of their significant economic, environmental, and social role. However, in recent years, they have faced increasing challenges due to climate change and human activities, which have directly affected their water resources. This study aims to evaluate the hydrological drought and vegetation cover trend in this region using remote sensing data, depending on the Land Surface Water Index (LSWI) and the Normalized Difference Vegetation (NDVI) index extracted from Sentinel 2 and Landsat satellite images during the period from 1984 to 2024. The results showed a strong relationship between hydrological drought and vegetation cover in the region. In 1984, approximately 30% of the study area was free of drought, with vegetation cover at around 41.1%. By 1994, severe and extreme drought conditions had spread to nearly 30% and 52, respectively of the total area of the region. This increase in drought intensity led to a sharp decline in vegetation cover to approximately 9.5%. Hydrological conditions have decreased by 2024, with no drought areas decreasing to nearly 6%. Vegetation cover recovered to only about 18.4%. This limited recovery of vegetation cover was linked to the persistence of extreme and severe drought conditions, which reached nearly 51% of the study area. The ongoing hydrological stress prevented vegetation cover from returning to the levels observed in 1984. Overall, the results confirmed the long-term environmental impacts of hydrological drought on the Iraqi marshes.

Keywords: GIS Hydrological Drought, Iraq's Marshes, LSWI, Remote sensing, Landsat images.

Drought is a recurring global natural disaster that covers extensive areas over prolonged periods, significantly impacting hydrology and ecosystems (Qaraghuli *et al.,* 2024). Drought results from insufficient precipitation and high evapotranspiration due to severe temperatures. It can be classified based on its impact on different sectors: a scarcity in rainfall leads to a meteorological drought, a decrease of soil moisture leads to an agricultural drought, deficits in water storage cause a hydrological drought, and socio-economic drought outcomes lead to food shortages and negative impacts on the agrarian economy. Droughts are among the severe natural disasters, affecting economies, populations, and agriculture (Rahman *et al.,* 2025). Since the 1980s, the drought related problems have been correlated with the recurring drought patterns. It is a slow-onset disaster with long-term impact on human and ecosystem activities, including food security, agriculture, health, biodiversity, energy, infrastructure, population displacement, water resources, land degradation, and economic development. The severity and occurrence of drought are closely correlate to the climatic conditions of the area (Radhi *et al.,* 2025). Drought increases in duration and intensity over a long period and has far-reaching effects. Researchers have come up with several definitions of this phenomenon, but the common denominators for all these definitions are water scarcity and dryness (Alahacoon & Edirisinghe, 2022). The increasing severity and frequency of drought require efficient methods for evaluating and monitoring drought states. Although available, traditional ground observations are frequently limited in temporal resolution and spatial coverage. Therefore, there is a growing dependence on remote sensing techniques and satellite

Article info - DOI: *https://doi.org/10.54386/jam.v28i2.3349*
Received:24 January 2026; Accepted: 21 May 2026; Published online : 04 June 2026

image indices to supply comprehensive and timely evaluations of drought intensity. Remote sensing provides a powerful tools for collecting large scale environmental data with high spatial resolution and temporal frequency (Ghobadi & Badehian, 2025). The collection of spatial information from satellite based imagery forms the foundation of remote sensing, enabling detailed evaluation of land cover properties, surface water, and vegetation distribution (Abood *et al.,* 2024). Complementing this approach, Geographic Information Systems (GIS) supply an integrated framework for organizing, visualizing, and analyzing geospatial data, thereby supporting effective decision making in a wide range of applications, especially in environmental disciplines (Khalaf & Abood, 2024). The Iraqi marshlands are a unique and ecologically significant wetland ecosystem. They have been vital to the cultural and economic life of the people (Almaarofi, 2015). The people of marshland regions were forced to leave their lands in the early 1990s due to drought. This led to significant wildlife and biodiversity loss, affecting regional and global scales (Jawad *et al.,* 2021). The marshlands faced challenges in providing a water supply due to anthropogenic impacts, particularly water shortage from 1993 to 2003. Quantifying the damage of drought is crucial for recovery plans (Al-Quraishi & Kaplan 2021). Although studies have addressed drought most have focused on climatic or agricultural indicators, while studies addressing hydrological drought using remote sensing techniques remain limited. Hence, the importance of this study, which aims to assess hydrological drought and variation in vegetation cover trend using the Land Surface Water Index (LSWI) and Normalized Difference Vegetation (NDVI) based on satellite data for the period 1984–2024 to provide an accurate picture of hydrological drought and vegetation cover changes in the Iraqi Marshlands.

MATERIALS AND METHODS

The research region is the southern marshes of Iraq, which are situated in the governorates of Basra, Missan, and Thi Qar and have an approximate area of 10,000 km^2. It is bounded between (46º 20’ 0″ E to 47º 25’ 0″ E) longitude and (30º 45’ 0″ to 31º 25’ 0″ N) latitude in UTM Zone 38N. This region is traditionally categorized into three major areas are Al-Hawizeh Marshes, Al-Hammar Marshes, and Central Marshes as shown in Fig. 1. The marshes in southern Iraq are divided into permanent, with distinct depressions that continue to retain floodwater, and seasonal, which receive floodwaters in the winter and evaporate this water in the hot summer months, and most of these marshes have clear heights relative to the permanent marshes (Al Ramahi *et al.,* 2024). The climatic conditions of the marshes region are distinguished by extreme thermal contrasts and arid characteristics. Summers are notably hot, with temperatures and evaporation frequently reaching to 38 C° and 494 mm, respectively. While in winter, temperature and evaporation can decline to approximately 12 C° and 61 mm, respectively, particularly in January. Precipitation levels are exceptionally low, with total annual rainfall generally remaining below 25 mm as shown in Table 1. The soil of the marshlands is fertile, containing heavy clay, silt, wet bogs, and water. The Euphrates and Tigris rivers are the main source of water in this area, as is the flow of many tributaries from Iran towards the Tigris and Hawiza (Irzoqy *et al.,* 2022). In this region, the groundwater depths range between about 1 meter and 30 meters, and it is not suitable for irrigation, as shown in Fig. 2 (Saleh *et al.,* 2020).

Data Used

Satellite imagery from Landsat sensors including the Multispectral Scanner (MSS, 1984), Thematic Mapper (TM, 1994), Enhanced Thematic Mapper Plus (ETM+, 2004), and Operational Land Imager (OLI, 2014) obtained from the USGS Earthexplorer platform (http://earthexplorer.usgs.gov), along with Sentinel 2 imagery for 2024 acquired from the Copernicus Data Space (https://dataspace.copernicus.eu), were used to evaluate environmental changes for the years 1984, 1994, 2004, 2014, and 2024 in the study area. To represent annual variability, a 12-month mean composite spanning January to December was used for each chosen year, allowing consistent monitoring of long-term dynamics in vegetation cover and surface water. All images were subjected to systematic digital pre-processing, including geometric correction to ensure spatial consistency, radiometric calibration to enhance data reliability, and atmospheric correction to minimize atmospheric interference. These processes were conducted by ERDAS Imagine 2014, ENVI 5.6, and ArcGIS 10.8 programs based analytical framework, ensuring the generation of standardized and dependable database. The processed imagery was subsequently analyzed to compute the Normalized Difference Vegetation Index (NDVI) and the Land Surface Water Index (LSWI), which were used to produce vegetation cover and hydrological drought maps, respectively. The combined interpretation of these indices enabled assessment of vegetation–water interactions, while spatial and temporal analyses were conducted to identify patterns, changes, and trends in vegetation condition and hydrological drought over the study period. The visual interpretation of images which were used with maps and the field survey by GPS device (during 19, 20, 21 and 22, October 2024) were used to validate the results (Fig. 3). Fig. 4 illustrates the methodology work which was conducted in this study.

Preprocessing and radiometric correction

The Sentinel-2 images from Level 2A were used, which are pre-corrected for atmospheric correction and were included in surface reflectance values, and therefore the study did not require any additional radiometric corrections to them. Moreover, Landsat satellite images, acquired at processing level 1, contain pixel values (digital numbers). These images required radiometric correction to accurately extract features from them. This processing is important for extracting meaningful data about the land covers in the study area. This process was performed by ENVI 5.6 software according to the equations from 1 to 3 (Pinto *et al.,* 2020), which are based on the MTL files (the metadata contents provided with the image). After completing the correction, the digital mosaic process was implemented to merge and unify the adjacent images of each platform into a single, continuous (Seamless) spatial frame, with the aim of covering the entire required geographical area without any gaps or variations in color and brightness. In the final stage, the study area was precisely subset-based on the approved geographical boundaries of the research, in order to focus analysis on the area of interest, reduce the size of the data, and prepare it for subsequent spatial analyses.

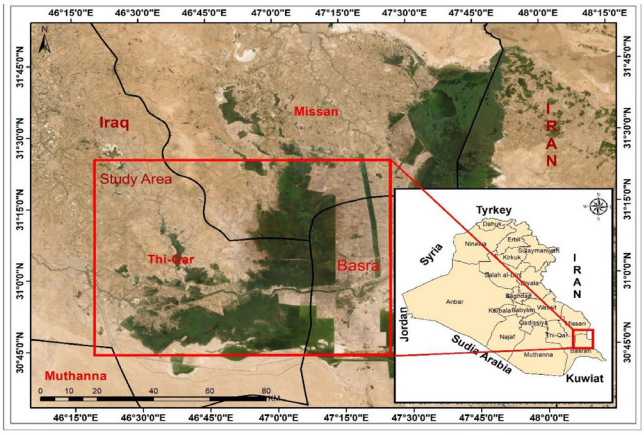

Fig. 1: Boundaries of the studied area

$$L_\lambda = M_L * Q_{cal} + A_L \quad (1)$$

Where: is the TOA spectral radiance; and are the band specific multiplicative and additive radiance rescaling factor, respectively (from the metadata); and is the calibrated and quantized standard product as digital numbers.

$$P\acute{\lambda} = M_P * Q_{cal} + A_P \quad (2)$$

Where:

Where: $P\acute{\lambda}$ is the TOA spectral reflectance; and are the band-specific multiplicative M_P and A_P additive reflectance rescaling factor, respectively (from the metadata); and Qcal is the calibrated and quantized standard product as digital numbers.

Then the reflectance value after sun angle correction was computed by:

$$P\lambda = \frac{P\lambda'}{\cos(\theta_{SZ})} = \frac{P\lambda'}{\sin(\theta_{SE})} \quad (3)$$

Where:

Pλ = TOA planetary reflectance

θ_{SE} = Local sun elevation angle

θ_{SZ} = Local solar zenith angle

Finally, Atmospheric correction was applied by ENVI program to convert the images from TOA reflectance values to surface reflectance values.

DROUGHT INDICES ADOPTED FOR EVALUATION IN THIS RESEARCH

In this research, two key drought indices were employed to evaluate drought conditions in the study area: Land Surface Water Index (LSWI), and the Normalized Difference Vegetation Index (NDVI) as follows:

Land surface water index (LSWI)

The LSWI is sensitive to the overall amount of liquid water in vegetation and its soil backdrop, and that liquid water strongly absorbs light in the SWIR (Chandrasekar et al., 2010). In order to evaluate drought, this index was developed based on the short wave infrared (SWIR) and near infrared (NIR) bands (Hadjimitsis *et al.,* 2010). It was proposed by Xiao *et al.,* (2004). The index is calculated according to the standard equation as follows (Zhang et al., 2013):

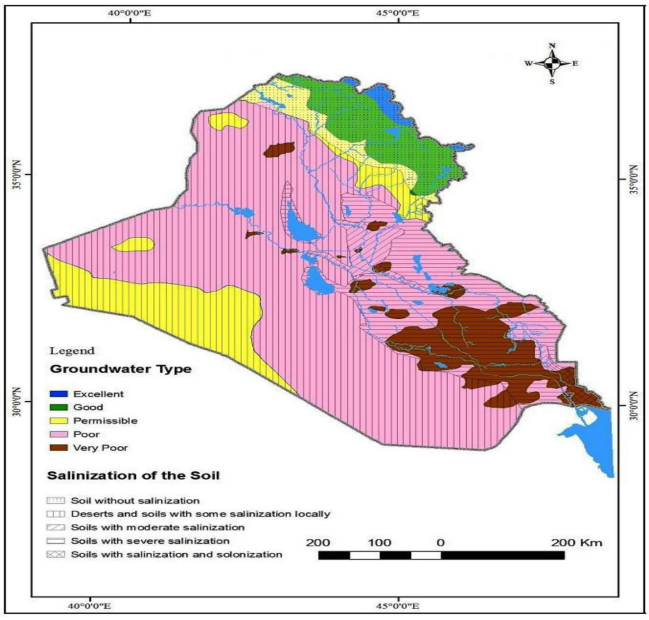

Fig. 2: Suitability of groundwater for irrigation purposes in Iraq (Saleh *et al.,* 2020)

$$LSWI = (R_{NIR} - R_{SWIR})/(R_{NIR} + R_{SWIR}) \quad (4)$$

A combination of SWIR and NIR bands was used to create the LSWI Index, which is sensitive to the amount of water in vegetation and land surface water due to the sensitivity of the SWIR band to soil moisture and vegetation water content. The reflectance of SWIR drops and its absorption increases with increasing soil moisture or vegetation water content, which raises LSWI values (Xiao *et al.,* 2006). Table 2 explains classes of LSWI drought index. In this study, the appropriate threshold for separating water from wetlands and drylands was determined based on the resulting values of the index and compared with available visual observations and field data.

Normalized difference vegetation Index (NDVI)

Vegetation indices are mathematical transformations of spectral reflectance values, especially in the near-infrared (NIR) and visible spectral bands. It is designed to extract vegetation properties such as water content, chlorophyll concentration, and canopy structure. Among these indices is the NDVI, which uses the variation in reflectance between the red and NIR bands to estimate vegetation health (Nitu *et al.,* 2025). The efficient monitoring of vegetation indicators by remote sensing techniques is beneficial for observing the vegetation changes around the world. (Awasthi *et al.,* 2022). The NDVI is an often-used index in vegetation satellite remote sensing, distinguishing healthy vegetation from soil, roads, senescent leaves,

Fig. 3: Samples of the field work in the study area

Table 1: Climate characteristics of the study area (1984-2024) (the Iraqi Meteorological and Seismology Organization and NASA's climate archives (https://power.larc.nasa.gov)

Month	Average rainfall (mm)	Average temperature (C°)	Average evaporation (mm)
January	22.3	12.2	61.8
February	15.2	15.1	85.7
March	20.4	21.2	158.3
April	11.1	26.3	218.1
May	4.2	32.1	344.6
June	0.0	37.2	467.4
July	0.0	38.1	494.6
August	0.0	38.4	456.1
September	0.5	34.3	347.1
October	5.3	28.2	220.2
November	21.1	20.1	103.4
December	21.4	14.3	75.5

Table 2: Classes of LSWI drought index (Du *et al.,* 2018)

Drought classes	Extreme	Severe and Moderate	Abnormally	No
Range	LSWI ≤ −0.1	-0.1 < LSWI ≤ 0	0 < LSWI ≤ 0.1	LSWI > 0.1

and buildings (Zhao & Qu, 2024). NDVI is dependent on variances in the red and near-infrared regions of the electromagnetic spectrum and it is computed by formula 5 as follows (Fathollahi *et al.,* 2024):

$$NDVI = \frac{NIR-Red}{NIR+Red} \quad (5)$$

Where Red and NIR represent to the spectral reflectance in the visible red and near-infrared regions of images, respectively. Its values range between +1 and -1. Higher positive values of NDVI, ranging from sparse plants or vegetation (0.1–0.5) to dense green vegetation (0.6 and above) (Fathollahi *et al.,* 2024).

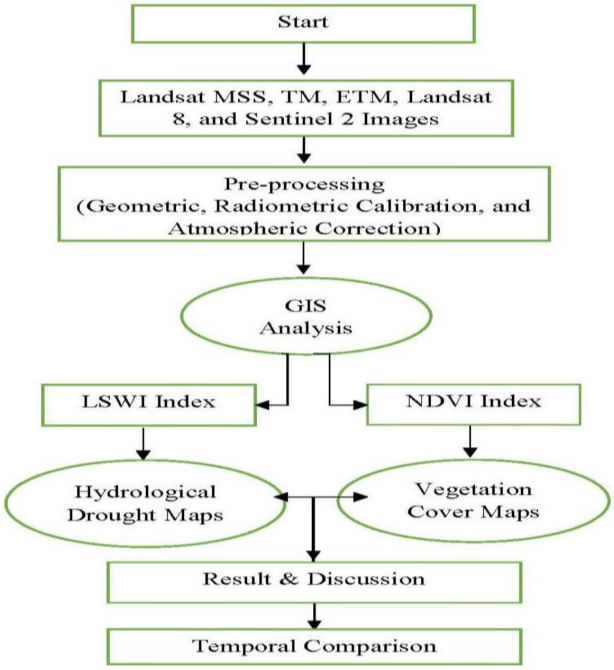

Fig. 4: Schematic diagram of methodology work applied in this study

RESULTS AND DISCUSSION

Analysis the relationships between NDVI and LSWI indices in the study area

The outcomes of the analysis of the relationship between the LSWI and NDVI indices showed a clear positive correlation across the different study years (Fig. 5). In 1984 (Fig. 5a), the strongest correlation between the two indices was recorded, with a correlation coefficient of R = 0.82, a coefficient of determination (R^2) of 0.67, and a root mean square error (RMSE) of 0.069. While, the strength of the relationship decreased relatively, with R = 0.74, R^2 of 0.54, and RMSE of 0.084 in 1994 (Fig. 5b). In 2004 (Fig.

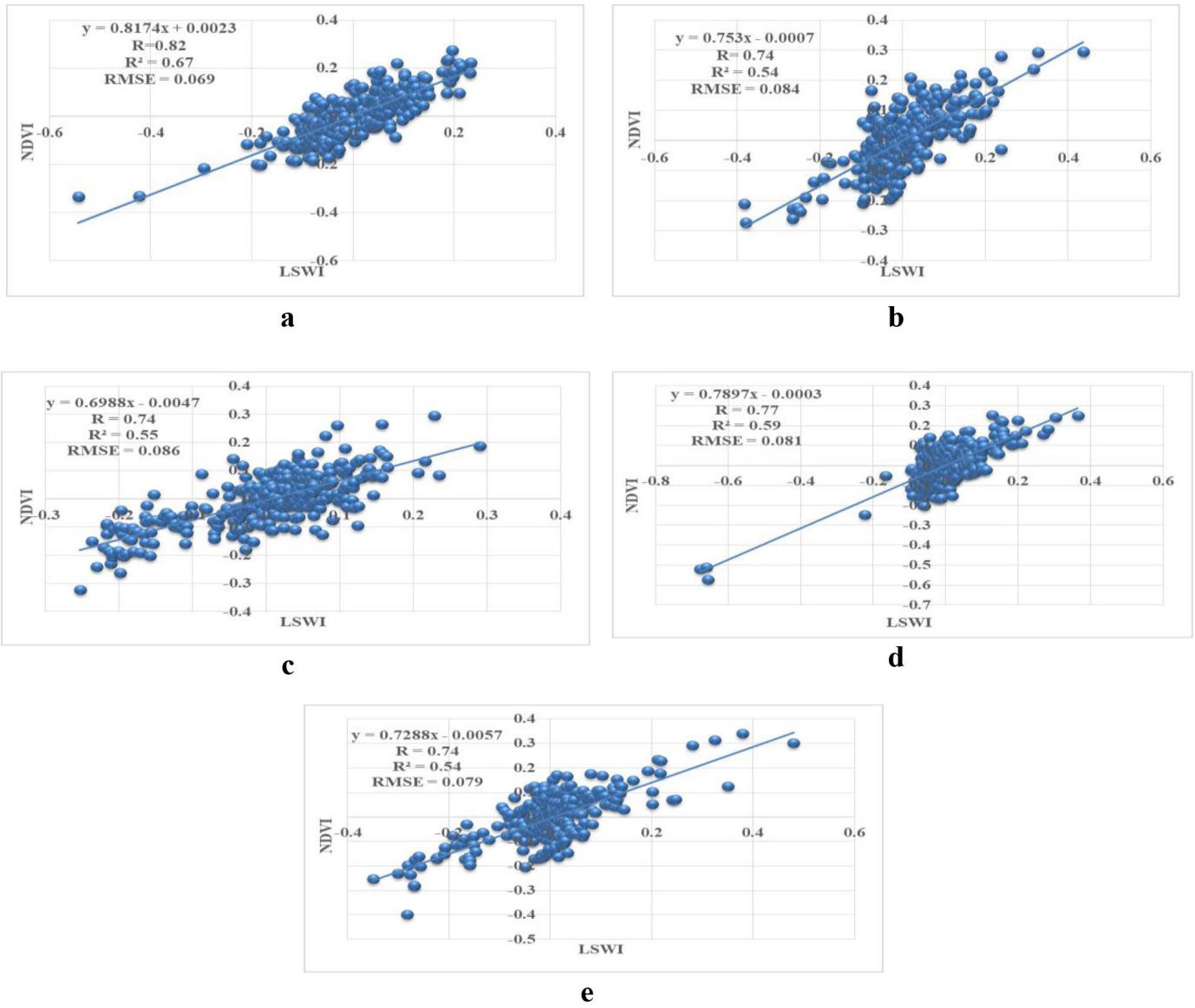

Fig. 5: The relationship between LSWI and NDVI indices in the study area (a) 1984, (b) 1994, (c) 2004, (d) 2014, and (e) 2024

Table 3: Percentage distributions of hydrological drought severity classes (1984-2024)

Hydrological drought	1984	1994	2004	2014	2024
Extreme	4	30	12	7	9
Severe	21	52	36	44	42
Moderate	27	11	22	19	28
Abnormally	18	4	22	5	15
No drought	30	3	8	25	6

Table 4: Percentage distributions of vegetation cover (1984-2024)

years	1984	1994	2004	2014	2024
Percentage	41.1	9.5	19.6	19.4	18.4

5c), the positive relationship between the two indicators persisted, with R = 0.74, R² of 0.55, and RMSE value of 0.086. Furthermore, in 2014 (Fig. 5d), the relationship strengthened again, with R = 0.77 and R² of 0.59, while the RMSE value decreased to 0.081. In 2024 (Fig. 5e), the positive relationship between the two indices continued, with R = 0.74, R² = 0.54, and RMSE value of 0.079.

Spatiotemporal of hydrological drought and vegetation cover trend

The spatiotemporal analysis of hydrological drought and vegetation cover in the Iraqi marshlands revealed significant environmental changes during the study period (1984–2024). Five years were selected to evaluate drought severity and vegetation dynamics using the LSWI and the NDVI indices in the study area.

Statistical analysis indicated there was positive relationship between the LSWI and NDVI indices for all study years, indicating that vegetation was highly dependent on water availability. The strongest relation was observed in 1984, reflecting stable hydrological conditions and abundant vegetation cover during this

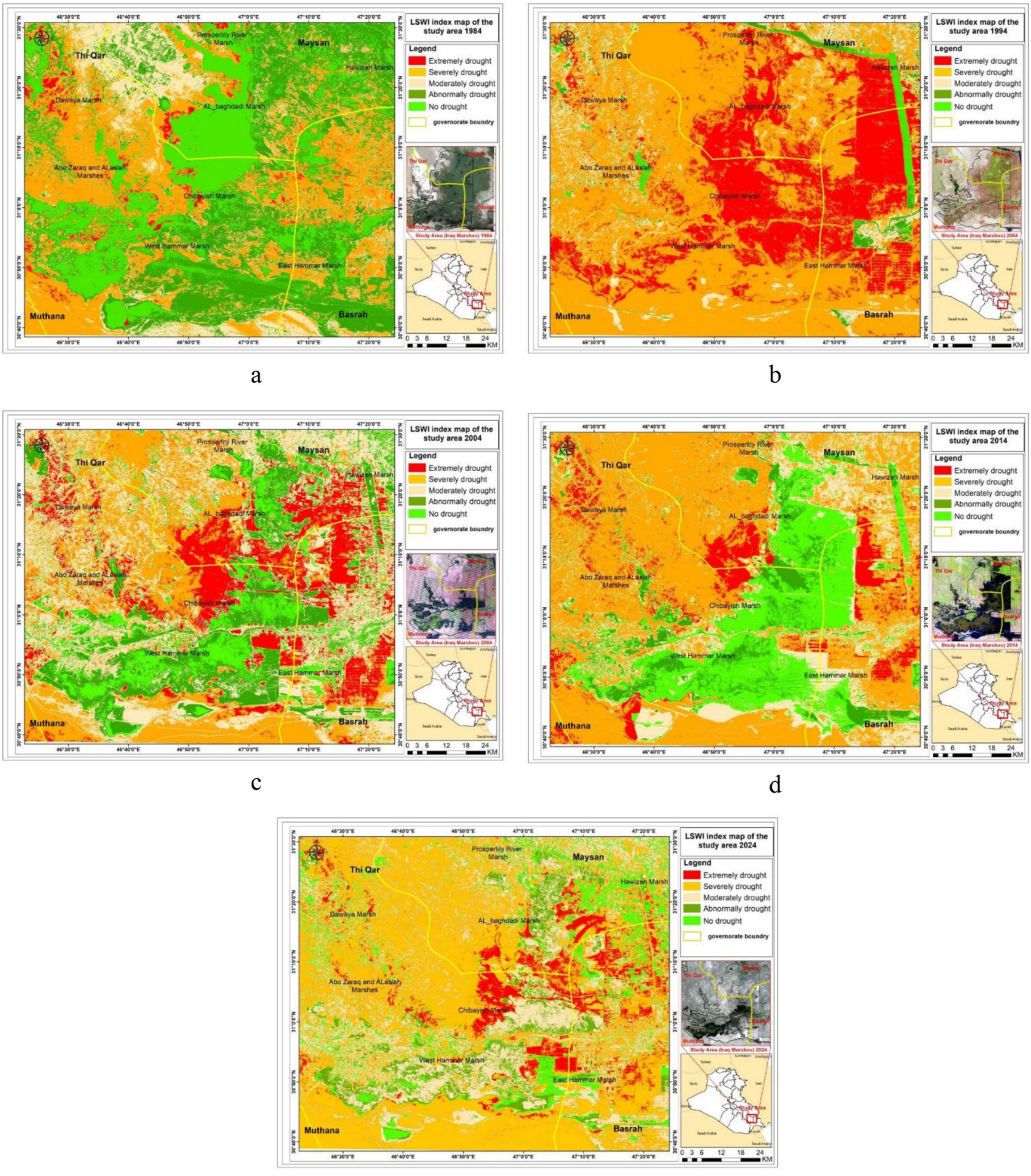

Fig. 6: Hydrological drought maps of the study area (a) 1984, (b) 1994, (c) 2004, (d) 2014, and (e) 2024

period. In 1994, the relation weakened slightly, coinciding with the severe drought conditions recorded during that year. This decrease in relation strength showed that hydrological stress negatively affected vegetation growth and reduced ecosystem resilience. The same values were recorded in 2004, showing the continued effect of drought on the wetland ecosystem. The relation enhanced again in 2014, which showed partial ecological recovery due to enhanced hydrological conditions. However, the relation weakened slightly in

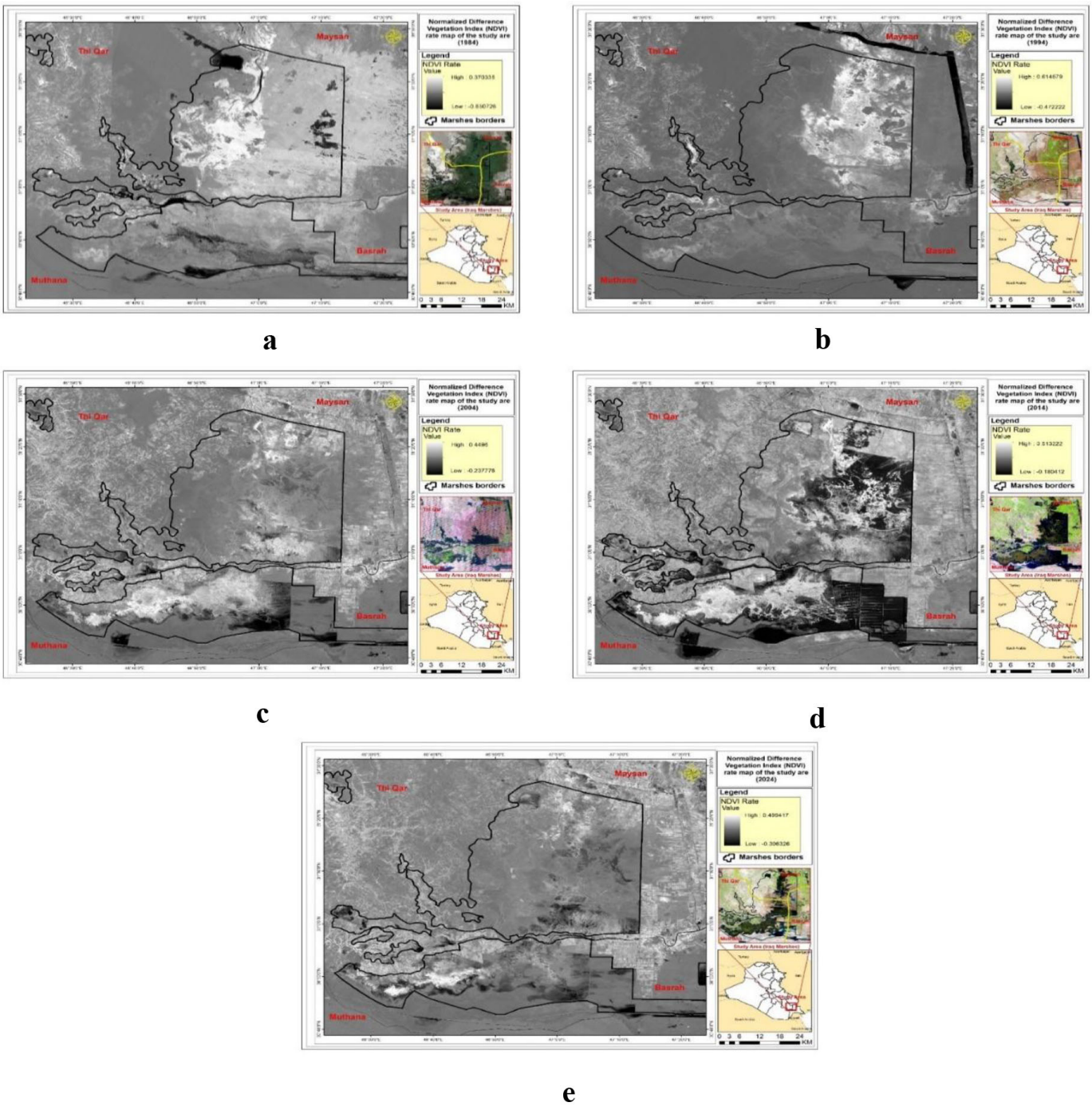

Fig. 7: Vegetation cover maps of the study area (a) 1984, (b) 1994, (c) 2004, (d) 2014, and (e) 2024

2024, confirming the continued effect of drought stress on wetland and vegetation cover distribution. These drought severity categories supported these results. The severe and extreme drought classes dominated large regions of the study area, especially in 1994, when severe hydrological drought accounted for about 52% and extreme drought for 30% of the overall area. Conversely, the percentage of no-drought regions decreased sharply from 30% in 1984 to only 3% in 1994, demonstrating the severity of hydrological drought during that period, as indicated in Fig. 6 and Table 3.

Although some enhancement was observed in 2014, with the percentage of no-drought areas increasing to 25%, hydrological drought states persisted until 2024, with severe hydrological drought still affecting 42% of the total area of the region. These fluctuations showed that wetlands were highly sensitive to climate changes and upstream water management practices. Although vegetation cover partially enhanced or recovered in subsequent years, reaching to

about 19.6% in 2004 and 19.4% in 2014, this percentage remained considerably lower than percentage of 1984. In 2024, vegetation cover decreased slightly again to about 18.4%, indicating continued environmental pressures and insufficient ecological recovery, as illustrated in Fig. 7 and Table 4.

Generally, the outcomes indicated that water scarcity has a direct impact on vegetation cover dynamics in the study area. The persistent decrease in vegetation cover and the widening range of drought severity classes highlight the combined impacts of climate changes, reduced river flow and human pressures on marsh sustainability. This is consistent with the outcomes of Irzoqy et al., (2022) and Al-Ansari (2025), which confirmed that climate changes, human pressures, and the policies of upstream countries (Iran and Turkey) represent an important factor in the degradation of the environmental states in the marshlands. These outcomes underscore the importance of integrated water resources management and ecological restoration strategies for the future preservation of the marsh ecosystem.

CONCLUSION

This study investigated four decades of hydrological drought behavior and associated vegetation changes in the Iraqi marshlands using multi-temporal remote sensing data spanning 1984 to 2024. The time-based analyses spanning 1984 to 2024 indicated a strong and direct correlation between increased hydrological drought and the declination of vegetation cover in the study area. In 1984, the region had remarkable environmental stability, with a 30% no-drought area, allowing for dense vegetation covering 41.1% of the total area. However, this balance changed entirely by 1994 as extreme and severe drought reached its peak of 30% and 52% respectively, leading to a decline of vegetation cover to about 9.5%. Water indicators gradually decreased by 2024, with the no-drought area at about 6%, vegetation showed a limited response and a faltering recovery at 18.4%. The inability of vegetation cover to recover to its original levels was mainly attributed to the dominance of the "extreme and severe droughts" pattern, which reached about 51% in 2024. This hydrological change has created an environment of continuous water stress that has prevented the return of vegetation to what it was four decades ago, with vegetation cover settling at 18.4% in 2024 compared to 41.1% in 1984.

ACKNOWLEDGEMENT

The authors acknowledge the School of Civil Engineering, Universiti Sains Malaysia for providing the necessary research facilities.

Author's certificate: The manuscript or its part is not under consideration for publication elsewhere and the same has been approved by all co-authors.

Conflict of Interests: The authors declare that there is no conflict of interest regarding the publication of this article.

Funding: No funding was received to assist with the preparation of this research.

Data Availability: The data that support the findings of this study are available from the authors, upon reasonable request.

Authors contribution: **Fadhaa Turki Dakhil*:*** Data curation, Formal analysis, and Writing-original draft, Methodology; **Nuridah Binti Sabtu**: Methodology, Investigation, review, editing, and Supervision; **Alaa G. Khalaf:** Investigation, Writing-review and editing, Formal analysis, Supervision.

Disclaimer: The contents, opinions, and views expressed in the research article published in the Journal of Agrometeorology are the views of the authors and do not necessarily reflect the views of the organisations they belong to.

Publisher's Note: The periodical remains neutral concerning jurisdictional claims in published maps and institutional affiliations.

REFERENCES

Abood, R. H., Mahdi, A. H., Khalaf, A. G., & Kadhim, A. A. (2024). Evaluation of land cover changes in Karbala governorate using remote sensing and GIS techniques. *Iraqi National Journal of Earth Science, 24*(2), 177–185. https://doi.org/10.33899/earth.2023.143323.1144

Alahacoon, N., & Edirisinghe, M. (2022). A comprehensive assessment of remote sensing and traditional based drought monitoring indices at global and regional scale. *Geomatics, Natural Hazards and Risk, 13*(1), 762–799. https://doi.org/10.1080/19475705.2022.2044394

Al-Ansari, N. (2025). Water resources in Iraq: Perspectives and prognosis. *Journal of Water Resources and Geosciences, 4*(1), 249–266.

Almaarofi, S. S. (2015). *Ecological assessment of re-flooded Mesopotamian marshes (Iraq)* (Ph.D. thesis). University of Waterloo.

Al-Quraishi, A. K., & David, A. K. (2021). Connecting changes in Euphrates River flow to hydropattern of the western Mesopotamian marshes. *Science of the Total Environment, 768*, 144445. https://doi.org/10.1016/j.scitotenv.2020.144445

Al Ramahi, F. K. M., Ali, A. B., & Rasheed, M. J. (2024). Remote sensing of climatic factors and the spectral reflectivity and their impact on the morphological characteristics of the Al-Hammar Marsh. *Iraqi Geological Journal, 57*(2E), 292–311. https://doi.org/10.46717/igj.57.2E.21ms-2024-11-30

Awasthi, N., Tripathi, J. N., Dakhore, K. K., Gupta, D. K., & Kadam, Y. E. (2022). Linkage between the vegetation indices and climate factors over Haryana. *Journal of Agrometeorology, 24*(4), 380–383. https://doi.org/10.54386/jam.v24i4.1834

Chandrasekar, K., Sesha Sai, M. V. R., Roy, P. S., & Dwevedi, R. S. (2010). Land surface water index (LSWI) response to rainfall and NDVI using the MODIS vegetation index product. *International Journal of Remote Sensing, 31*(15), 3987–4005. https://doi.org/10.1080/01431160802575653

Du, T. L. T., Bui, D. D., Nguyen, M. D., & Lee, H. (2018). Satellite-based, multi-indices for evaluation of agricultural droughts in a highly dynamic tropical catchment, central Vietnam. *Water, 10*, 659. https://doi.org/10.3390/w10050659

Fathollahi, L., Wu, F., Melaki, R., Jamshidi, P., & Sarwar, S. (2024). Global normalized difference vegetation index forecasting from air temperature, soil moisture and precipitation using a deep neural network. *Applied Computing and Geosciences, 23*, 100174. https://doi.org/10.1016/j.acags.2024.100174

Ghobadi, M., & Badehian, Z. (2025). Assessment of agricultural drought severity using multi-temporal remote sensing data in Lorestan region. *Scientific Reports, 15*, 18528. https://doi.org/10.1038/s41598-025-03087-4

Hadjimitsis, D. G., Papadavid, G., Agapiou, A., Themistocleous, K., Hadjimitsis, M. G., Retalis, A., Michaelides, S., Chrysoulakis, N., Toulios, L., & Clayton, C. R. I. (2010). Atmospheric correction for satellite remotely sensed data intended for agricultural applications: Impact on vegetation indices. *Natural Hazards and Earth System Sciences, 10*, 89–95. https://doi.org/10.5194/nhess-10-89-2010

Irzoqy, I. M. M., Ibrahim, L. F., & Al-Tufaily, H. M. A. (2022). Analysis of the environmental reality of the marshes and its sustainable development. *IOP Conference Series: Earth and Environmental Science, 1002*, 012010. https://doi.org/10.1088/1755-1315/1002/1/012010

Jawad, L., Salim, M., & Abed, S. (2021). *The southern marshes of Iraq*. In *Southern Iraq's marshes: Their environment and conservation*. Springer.

Khalaf, A. G., & Abood, R. H. (2024). Evaluation of groundwater quality in Najaf and Hilla area of Iraq based on weighted arithmetic method and GIS. *AIP Conference Proceedings, 3105*(1). https://doi.org/10.1063/5.0212629

Nitu, A., Florea, C., Ivanovici, M., & Racoviteanu, A. (2025). NDVI and beyond: Vegetation indices as features for crop recognition and segmentation in hyperspectral data. *Sensors, 25*, 3817. https://doi.org/10.3390/s25123817

Pinto, C. T., Jing, X., & Leigh, L. (2020). Evaluation analysis of Landsat Level-1 and Level-2 data products using in situ measurements. *Remote Sensing, 12*(6). https://doi.org/10.3390/rs12162597

Qaraghuli, K., Murshed, M. F., Said, M. A. M., Mokhtar, A., & Rousta, I. (2024). Univariate and multivariate imputation methods evaluation for reconstructing climate time series data: A case study of Mosul Station-Iraq. *Journal of Agrometeorology, 26*(3), 318–323. https://doi.org/10.54386/jam.v26i3.2657

Radhi, F. M., Khalil, S. M., & Ali, S. A. (2025). Drought monitoring using remote sensing-based indices in the southern region of Iraq. *International Journal of Geoinformatics, 21*(6). https://doi.org/10.52939/ijg.v21i6.4227

Rahman, G., Khalid, S., Arshad, S., Moazzam, M. F. U., & Kwon, H. H. (2025). Remote sensing-based spatiotemporal assessment of agricultural drought and its impact on crop yields in Punjab, Pakistan. *Scientific Reports, 15*. https://doi.org/10.1038/s41598-025-06095-6

Saleh, S. A., Al-Ansari, N., & Abdullah, T. (2020). Groundwater hydrology in Iraq. *Journal of Earth Sciences and Geotechnical Engineering, 10*(1), 155–197.

Xiao, X., Zhang, Q., Braswell, B., Urbanski, S., Boles, S., Wofsy, S., Moore, B., III, & Ojima, D. (2004). Modeling gross primary production of temperate deciduous broadleaf forest using satellite images and climate data. *Remote Sensing of Environment, 91*(2), 256–270.

Xiao, X., Hagen, S., Zhang, Q., Keller, M., & Moore, B. (2006). Detecting leaf phenology of seasonally moist tropical forests in South America with multi-temporal MODIS images. *Remote Sensing of Environment, 103*(4), 465–473. https://doi.org/10.1016/j.rse.2006.04.013

Zhang, N., Hong, Y., Qin, Q., & Zhu, L. (2013). Evaluation of the visible and shortwave infrared drought index in China. *International Journal of Disaster Risk Science, 4*(2), 68–76. https://doi.org/10.1007/s13753-013-0008-8

Zhao, Q., & Qu, Y. (2024). The retrieval of ground NDVI (normalized difference vegetation index) data consistent with remote-sensing observations. *Remote Sensing, 16*, 1212. https://doi.org/10.3390/rs16071212